

UNCLASSIFIED

Defense Technical Information Center
Compilation Part Notice

ADP011175

TITLE: Active Optimisation of the Performance of a Gas Turbine
Combustor

DISTRIBUTION: Approved for public release, distribution unlimited

This paper is part of the following report:

TITLE: Active Control Technology for Enhanced Performance Operational
Capabilities of Military Aircraft, Land Vehicles and Sea Vehicles
[Technologies des systemes a commandes actives pour l'amelioration des
performances operationnelles des aeronefs militaires, des vehicules
terrestres et des vehicules maritimes]

To order the complete compilation report, use: ADA395700

The component part is provided here to allow users access to individually authored sections
of proceedings, annals, symposia, etc. However, the component should be considered within
the context of the overall compilation report and not as a stand-alone technical report.

The following component part numbers comprise the compilation report:

ADP011101 thru ADP011178

UNCLASSIFIED

ACTIVE OPTIMISATION OF THE PERFORMANCE OF A GAS TURBINE COMBUSTOR

M. M. Miyasato, V. G. McDonell, and G. S. Samuelsen

UCI Combustion Laboratory, Bldg. 323, Room 221

University of California

Irvine, CA 92697-3550, USA

(949) 824-5950 gss@uci.edu

ABSTRACT

The increasingly stringent regulation of gas turbine exhaust emissions, combined with the need to reduce overall cost of operation, is requiring advancements to be made in the combustion system. In particular, the ability of these systems to attain both low emissions and high efficiency over increasingly longer periods of operation, in order to reduce maintenance costs, is requiring new thinking with respect to the system control strategies. This new thinking is further necessitated by operation of these devices at conditions that are prone to combustion instabilities. As a result, development of a gas turbine that can actively respond to changes in load, system wear, and/or fuel composition, while maintaining efficiency and emissions performance, would be well received. Many technological hurdles must be overcome for this to occur, including the development of sensors, control strategies, and hardware capable of “self-tuning” or “active optimization.”

In the present study, a model natural gas-fired industrial gas turbine combustor is utilized to evaluate the performance of different active optimization strategies. Sensors for exhaust species and reaction zone chemiluminescence are utilized in conjunction with an adaptive fuel injection strategy in a closed loop control system. This system has been developed to maintain overall performance in light of environmental changes (e.g., fuel composition changes, injector wear, load changes). The feedback sensor consists of traditional extractive probe based exhaust measurements of major species including carbon monoxide and oxides of nitrogen. This sensor is utilized to provide direct measurement of emissions performance in terms of CO and NO_x emissions. Chemiluminescence is utilized to evaluate the ability of inferential methods to provide very fast, yet accurate indicators of performance. For the current study, a simulated injector perturbation scenario (partial fuel jet blockage) is utilized to examine the robustness of the different optimization strategies. And, as a first step, a direction-set algorithm is utilized to search for the region of optimal performance. The results obtained illustrate (1) the relative correlation of the different sensor strategies with system performance, and (2) the ability of the closed loop control to maintain combustion performance in light of an unexpected hardware perturbation.

INTRODUCTION

Due to increasingly stringent emissions regulations for industrial, stationary combustion sources, low emissions technologies are relying more and more on lean, well-mixed or premixed strategies.

These strategies, although proficient at reducing NO_x emissions, suffer from reduced stability or decreased system efficiency under operating conditions which are often desirable for low emissions; as a result, high performance operation can present operational and safety challenges. An attractive technology to address these challenges is the application of *active optimization* of the combustion process using feedback sensors, an optimization algorithm, and computer control of the combustor. Major challenges associated with conducting this type of adaptive optimization on industrial combustion systems are identifying (1) parameters amendable for control, (2) reaction characteristics appropriate for feedback sensing, (3) sensor and control time response requirements, and (4) low maintenance and cost impacts. This study investigates the applicability of adaptive fuel injection to stationary gas turbines in relation to these challenges and over several operational scenarios.

Active control of gas turbines has been studied using dynamic control of the fuel injection to offset combustion instabilities (e.g. Neumeier and Zinn, 1996; Hong, et al., 1998). An alternative strategy is to tailor the fuel and air mixing in order to (1) minimize emissions and (2) avoid instabilities; the amount of mixing has been shown to significantly effect the emissions (Appleton and Heywood, 1973, and Lyons, 1981) as well as stability (Shih et al, 1996). The research addressed in this paper investigates this latter strategy, i.e., to minimize emissions by actively controlling the spatial fuel and air mixedness such that high performance is achieved despite changes in load (equivalence ratio) or hardware degradation. Toward this end, a novel fuel injection strategy is applied to provide sufficient, flexible, and simple control over the entire turndown or duty cycle range of the gas turbine. The active optimization strategy is tested over the stability range of the combustor and then under a simulated hardware degradation or unexpected perturbation mode, where two injector fuel jets are partially blocked.

In order to respond rapidly to unexpected changes, fast feedback sensors are required. Previous work identified the need for such feedback control in order to attain and maintain high performance under changing load conditions (St. John and Samuelsen, 1994; Davis and Samuelsen, 1996; Jackson and Agrawal, 1999). These fast sensors would be situated near the reaction, thereby avoiding the long convection times associated with exhaust sampling, and would therefore provide faster optimization, reduced emissions even during load cycling, and, if possible, stability information. These feedback sensors will most likely be optical in order to provide the fast time response required. As a first step toward this

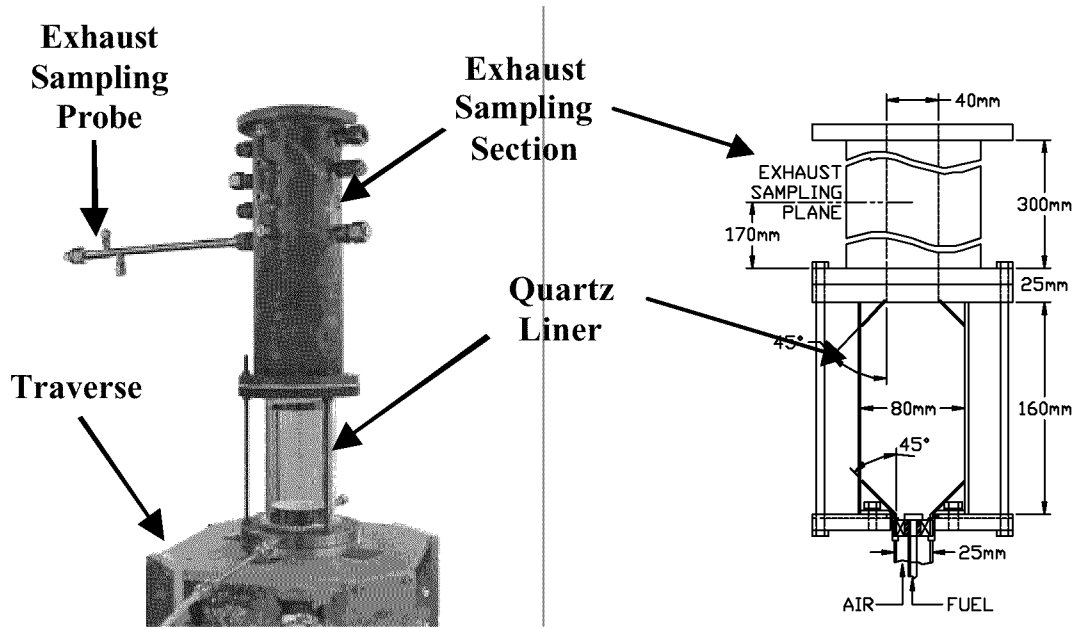


Figure 1: Atmospheric Test Facility

goal, flame chemiluminescence is used to assess its ability to accurately reflect the emissions performance.

OBJECTIVES AND APPROACH

The objectives of the current study are to assess the viability and degree of success of (1) flexible spatial mixing strategy for performance control, (2) the use of flame chemiluminescence as a fast, inferential sensor for faster feedback, and (3) the robustness of the adaptive control strategy over the entire operability range and under a simulated perturbation mode.

A four step approach was utilized in the current study—(1) measure the NO_x , CO, and chemiluminescence emissions over the entire operability range of the model combustor, (2) identify the regions of optimal performance (in terms of low NO_x and CO), (3) apply and compare active control using the chemiluminescence sensor to the conventional emissions analyzers, and (4) simulate a hardware perturbation by blocking two injector jets and apply active control to assess the systems response.

EXPERIMENT

The test facility utilized provides a wide range of operating conditions and flow metering. The test stand is designed to operate at 1 atm with inlet temperatures up to 800 K. The model combustor test rig, shown in Figure 1, has a quartz liner to allow optical access for reaction visualization and chemiluminescence measurements.

Model Combustor

The model combustor utilizes two independent natural gas injection circuits to tailor the fuel distribution. The first fuel circuit injects the fuel radially from the centerbody into the swirling air stream. This centerbody injection circuit, labeled “CB” in Figure 2, consists of six equally spaced fuel holes located circumferentially along the side of the fuel manifold. The fuel manifold is positioned directly

above the swirler hub. The second fuel injection circuit allows fuel to be injected radially inward from the surrounding wall. This wall injection circuit, labeled “WJ” in Figure 2, consists of six equally spaced fuel holes in positions that are staggered with respect to the centerbody injection holes. By varying the fuel split between the two fuel circuits, a variety of fuel distributions can be achieved (Flores et al, 2000).

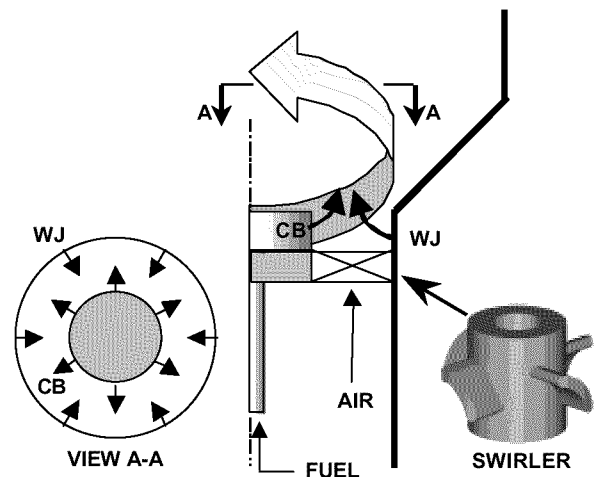


Figure 2: Detail of Fuel Injection Options.

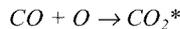
The baseline configuration is a four vane axial swirler. The nominal firing rate for the system is 15 kW of natural gas at 0.0093 kg/sec of air, though the fuel flow rates were varied to assess the system’s performance. An air inlet temperature of 700 K was utilized in all cases.

Diagnostics

Since the general objective of the optimisation strategy is to mitigate exhaust gas pollutants, a direct measure of the pollutants is warranted. Exhaust emissions were collected via a 12.7 mm diameter, water-cooled, stainless steel extractive probe. This emissions probe is used to sample the exhaust emissions downstream of the exit plane of the combustor, as shown in Figure 1. This probe is designed to take an integrated average measurement of the emissions over the diameter of the sampling plane. The water in the probe is heated to 325 K to protect the probe and quench the sample while avoiding condensation of water vapor inside the probe. The emissions are pumped through a heated Teflon line to prevent water condensation. The sample stream goes through a converter to reduce any NO_2 to NO prior to the water drop out. After the water drop out, the exhaust gas is delivered to a portable emissions analyzer (Horiba Ltd. model PG250A), which measures carbon monoxide (CO), carbon dioxide (CO_2), oxygen (O_2), and nitrogen oxides (NO_x).

Although the measurement of the combustor exhaust emissions provides a direct indication of the performance, a more convenient strategy with much faster time response is desirable, and likely necessary in order to optimize performance and maintain stable combustion. An optimisation strategy based on an indirect measure must then estimate the associated combustion performance. Two strategies were investigated, acoustics and reaction chemiluminescence. While the acoustic measurements yielded some potentially useful results, they were not very robust and additional work is required to attain the desired performance. As a result, only the results from the chemiluminescence investigations are presented here. For the chemiluminescence, three radial species were considered: OH, CH, and CO_2^* . Initial studies were conducted using a polychromator, and the overall signal levels associated with the CO_2^* chemiluminescence were found to be much greater than those were for OH or CH. As a result, the detailed characterizations were conducted using CO_2^* .

The basic setup for the chemiluminescence utilized a 200 μm core fiber located approximately 49 cm away from the combustor to allow the 14° expansion of the fiber to encompass the entire reaction volume. The fiber end is attached to a collimating lens, which directs the signal through an appropriate filter and then to a photomultiplier tube (PMT). In the case of CO_2^* , a 310-600 nm bandpass filter is utilized to capture the CO_2 continuum. For the system studied, the CO_2^* chemiluminescence,



provided an intense and measurable signal over the entire operability range of the combustor. The data values are sampled at a rate of 25000 Hz over 3 seconds. The chemiluminescence has the other obvious advantage in that it could potentially be utilized as an instantaneous reaction monitor, thereby providing an indication of the reaction stability. In this case, additional sampling issues must be addressed.

The basic setup for the direct emissions and chemiluminescence setup is shown schematically in Figure 3. As a result, both direct and estimated performance are determined for the combustor.

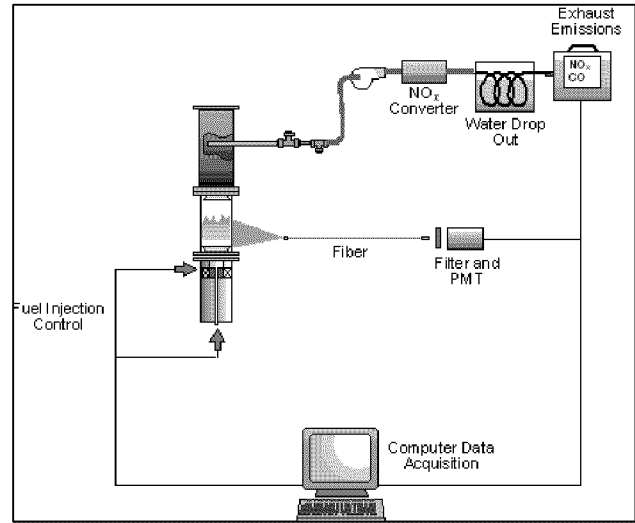


Figure 3: Model Gas Turbine Diagnostics and Control Setup

Active Optimization

The active optimization strategy utilizes a simple hill climbing, or direction-set, methodology for the search algorithm while trying to continually increase or optimize performance in terms of NO_x and CO emissions. In order to quantify performance and deal objectively with the trade-off that often occurs between NO_x and CO, a cost function is defined:

$$J = w_{\text{NO}_x} f(\text{NO}_x) + w_{\text{CO}} g(\text{CO})$$

where w_{NO_x} and w_{CO} are weighting functions. The definitions and plots of the functions $f(\text{NO}_x)$ and $g(\text{CO})$ are shown below:

$$f(\text{NO}_x) = \begin{cases} 1 - 0.75 \cdot \left(\frac{[\text{NO}_x]}{5} \right)^4 & , [\text{NO}_x] \leq 5 \text{ppm} \\ (1 - 0.75) \cdot \frac{[\text{NO}_x]_{\text{max}} - [\text{NO}_x]}{[\text{NO}_x]_{\text{max}} - 5} & , [\text{NO}_x] > 5 \text{ppm} \end{cases}$$

$$g(\text{CO}) = \begin{cases} 1 - 0.90 \cdot \left(\frac{[\text{CO}]}{8} \right)^4 & , [\text{CO}] \leq 8 \text{ppm} \\ (1 - 0.90) \cdot \frac{[\text{CO}]_{\text{max}} - [\text{CO}]}{[\text{CO}]_{\text{max}} - 8} & , [\text{CO}] > 8 \text{ppm} \end{cases}$$

The performance, J , therefore increases with decreasing NO_x and CO, i.e., good performance.

The search algorithm uses the performance index to comparatively seek out conditions of higher performance. The algorithm controls the combustor by varying the two fuel inputs (centerbody and wall jets) to affect the fuel split and equivalence ratio. The feedback sensors provide the information necessary to calculate the performance parameter, J , at each condition. The algorithm proceeds along a certain direction until J is no longer maximized. The algorithm then simply chooses a new direction at a predetermined angle and step size. If the new condition has a higher performance index then the algorithm proceeds in the new direction; if the performance is not higher, another new angle rotation is selected, and so on. For the present study, the functions of NO_x and CO are equally weighted.

RESULTS

Baseline Configuration

In order to establish the research baseline and know whether the active optimization was successful, exhaust emissions and chemiluminescence measurements were taken over the model combustor’s entire operational space. The NO_x and CO emissions were then used to calculate the performance, J , as described previously. The resulting performance map is shown in Figure 4 (in all of the subsequent similar figures, the y-axis represents the fuel split as a percentage of fuel injected through the centerbody jets and the x-axis represents the equivalence ratio). The region of peak performance is located in the ridge along 0.42 equivalence ratio and between fuel splits 20-60%. The plot shows that the performance is relatively insensitive to the fuel split, giving rise to the large region of high performance at the 0.42 equivalence ratio.

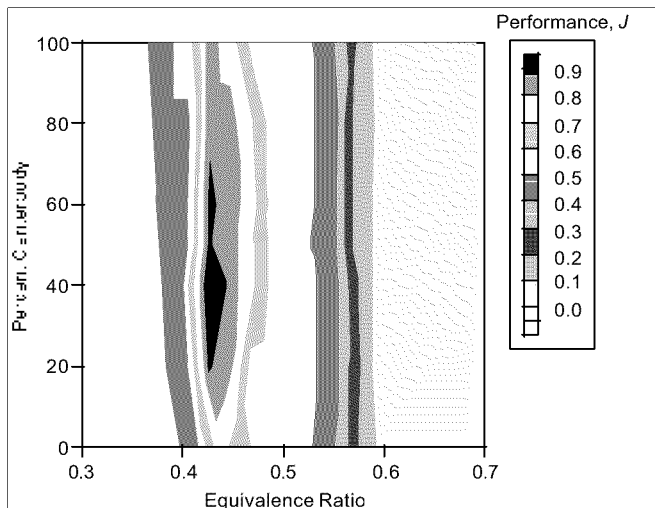


Figure 4: Performance Map for Model Gas Turbine Combustor based on Emissions.

The active optimization control system was applied to the model combustor using the emissions analyzers as the feedback sensors. The resulting search path is shown overlaid on the performance map in Figure 5. The combustor was started at a poor performing condition and allowed to optimize, finishing very near the absolute peak performance condition. The search took 21 iterations and 28 minutes to settle on the optimum ridge.

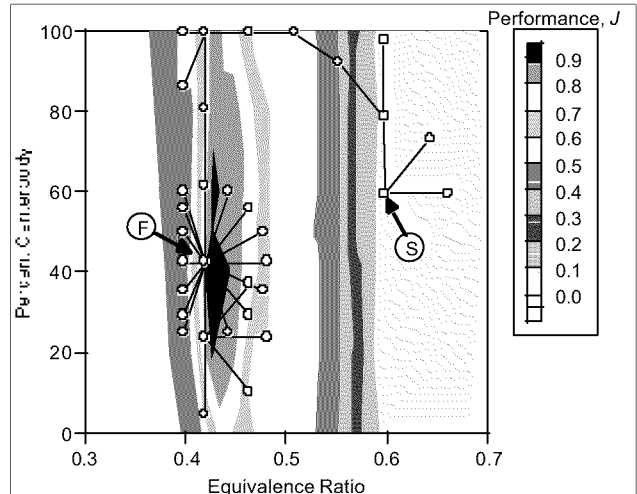
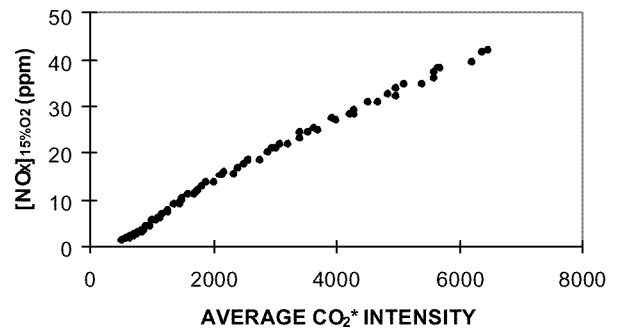


Figure 5: Active Optimization History Using Emissions Analyzers
 (S) = starting and (F) = finishing condition

In order to reduce the optimization time, CO_2^* chemiluminescence measurements were enlisted. Correlations were developed to relate the average CO_2^* signal to the exhaust NO_x concentration and the percent fluctuating CO_2^* signal to the exhaust CO emissions (Figure 6).

a) NO_x Correlation and Average Chemiluminescence Signal



b) CO Correlation with % Fluctuation of Chemiluminescence

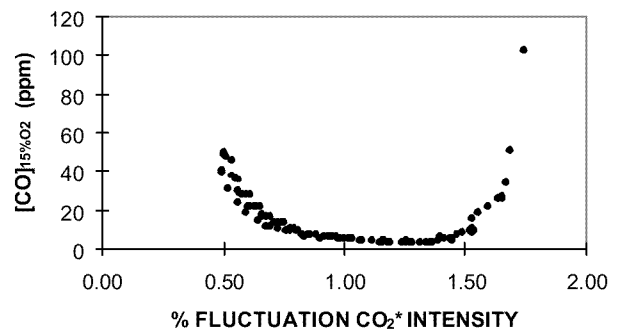


Figure 6. Exhaust Emissions Correlation with Chemiluminescence.

Based on the correlations shown in Figure 6, the optimization process was revisited with the chemiluminescence based feedback (i.e., estimation) for performance incorporated into the active optimization system. The resulting search is shown in Figure 7.

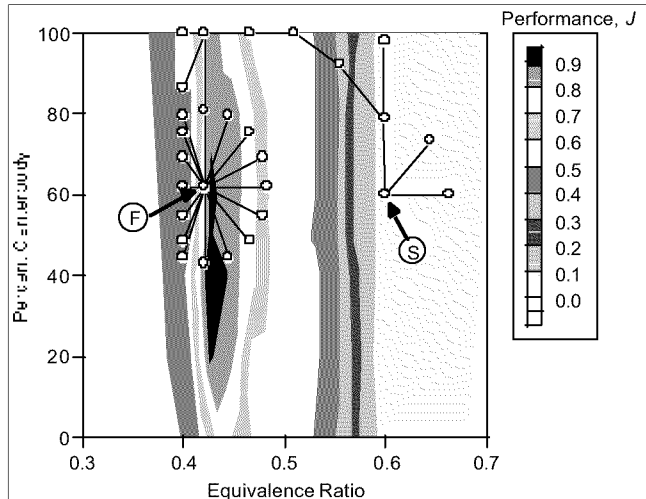


Figure 7: Active Optimization History Using CO_2^*

Although the chemiluminescence feedback optimized on a slightly different fuel split than the emissions feedback; the difference in performance index is only about 0.002. Furthermore, the chemiluminescence was able to optimize at a much faster rate, 4 times faster than the emissions feedback case. In fact, the response of the sensor was sufficient to allow even faster optimization, however, the time constant associated with the overall system establishes a reasonable limit. Indeed, this aspect of the system dynamical control for optimization of performance requires careful consideration in the development of actuation and control algorithms. If the controller is too aggressive, damage may result.

As shown in Figure 7, the active optimization strategy employed using flexible fuel injection and two different feedback sensors (emission analyzers and reaction chemiluminescence) was able to successfully identify the regions of highest performance, with the chemiluminescence feedback offering much faster time response. The next test was to determine the robustness of the system by applying a large change to the system hardware.

Partially Block Injector

In order to provide a scenario with which to evaluate the utility of the sensor and optimization strategies, the fuel injector was perturbed by partially blocking two adjacent centerbody fuel injection jets. In practice, such wear and tear may occur gradually, or, in the case of the ingestion of a foreign object, a rather sudden obstruction may occur. Also, scenarios where fuel compositional changes may occur and lead to variation in performance which could then be improved in real time can be envisioned (e.g., Flores, et al., 2000). For the case of the present evaluation, the partially block injector scenario was utilized to provide a significant change in performance as an “extreme” case. Figure 8 illustrates the strategy utilized in the partial blocking. Basically, two adjacent fuel holes on the centerbody were partially blocked.

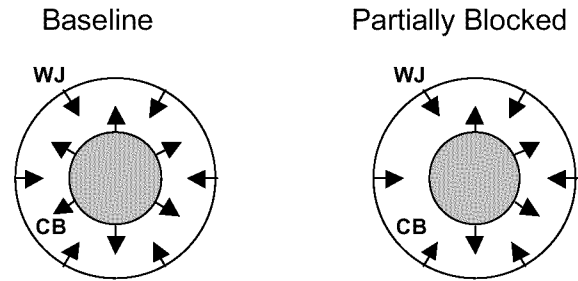
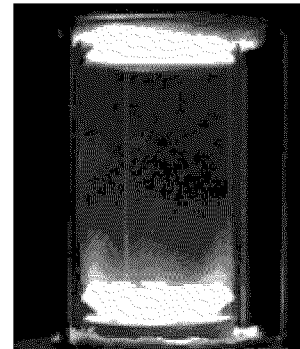


Figure 8. Partially Blocked Centerbody.

This asymmetrical blockage resulted in an altered flame structure compared to the baseline configuration as shown in Figure 9. The difference in centerbody injector pressure drop causes more fuel injection and higher temperatures along the left side of the liner.

a) Baseline Injector



b) Partially Blocked Injector

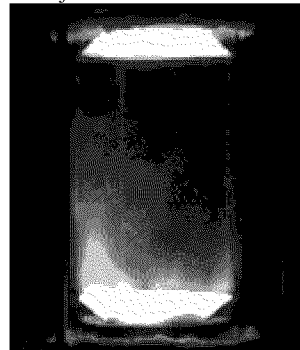


Figure 9: Reaction Structures at $CB=60\%$ $\phi=0.60$

To illustrate the impact the partially blocked injector has on the fuel distribution, Figure 10 presents the fuel distributions measured immediately downstream of the centerbody (see Figure 2). Figure 10a reveals that the baseline case exhibits periodic peaks in fuel concentration due to the discrete jets. The apparent asymmetry shown in the baseline case is associated with the location of the fuel jet and the orientation of the axial swirler. The behavior of the fuel jet depends upon the relative wake effect behind the four vanes (Flores, et al., 2000). In the case of the partially blocked injector, shown in Figure 10b, the fuel distribution is clearly skewed to one side of the combustor. In this case, the variation associated with vane wakes appears to be overshadowed by the local increase in

fuel due to the two partially blocked holes. Given the rather significant impact on the fuel distribution, the visible reaction structure changes shown in Figure 9 appear relative minor. As a result of the partial blockage, some performance changes were expected. The resulting performance map is shown in Figure 11, and does indeed show major changes. Again, the changes in performance are significant given the relatively minor visible differences in reaction structure shown in Figure 9.

The performance contour plot shows a “valley” at high centerbody fuel ratios. This result is due to the asymmetric centerbody fuel injection and the resulting higher NO_x levels. The optimum conditions subsequently occur at higher wall jet ratios but at the same equivalence ratio (0.42) as in the baseline, unblocked case. The maximum performance values, however, are less than for the unblocked condition. Nevertheless, the active optimization strategy was initiated on this hardware configuration, starting at the optimized condition for the baseline case. This scenario represents an unexpected hardware perturbation from sudden hardware failure or the ingestion of a foreign object inside the combustor.

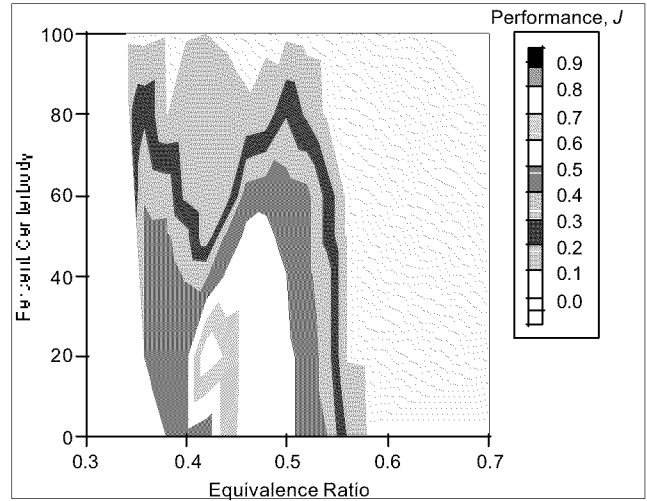


Figure 11: Performance Map for Partially Block Injector based on Exhaust Emissions.

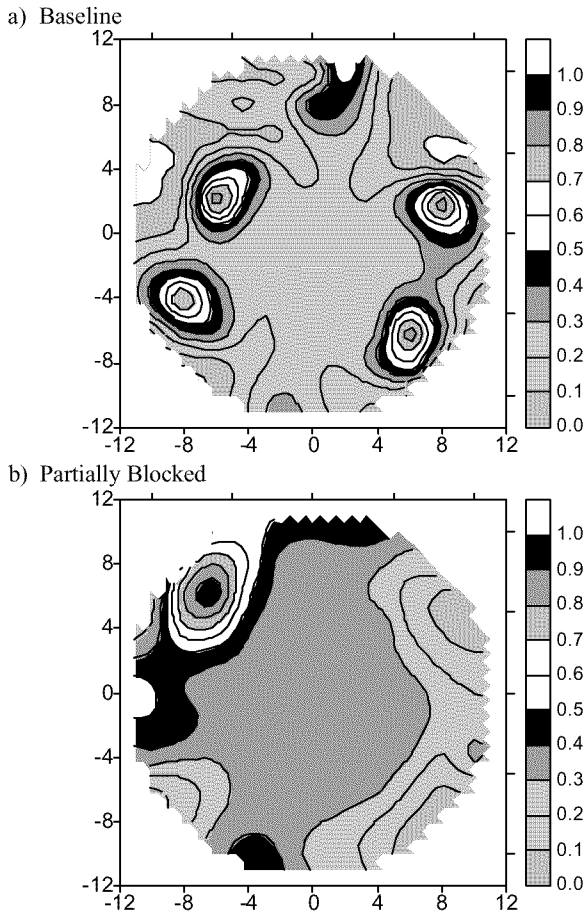


Figure 10. Fuel Distribution 3 mm Downstream of Centerbody.

The active optimization histories using the emissions feedback and CO_2^* chemiluminescence are shown in Figure 12. The search paths for both optimizations are identical but the chemiluminescence feedback is able to optimize 2.7 times faster than when using emissions feedback.

Thus, the active optimization strategy using the flexible fuel injection and either emissions or chemiluminescence feedback was successful in locating the maximum performance conditions even under degenerated hardware configurations. The chemiluminescence feedback, as in the baseline configuration, provided much faster response and optimization.

It should be noted that the performance contour plot illustrated for the chemiluminescence feedback, Figure 12 (b), represents the *inferred* performance based on the chemiluminescence values. Although careful curve fits were conducted for multiple fuel splits for the range of equivalence ratios, some scatter in the data resulted in differences between the inferred performance [Figure 12(b)] and the emissions-based performance [Figure 12(a)]. These differences and their implications are addressed further in the following section.

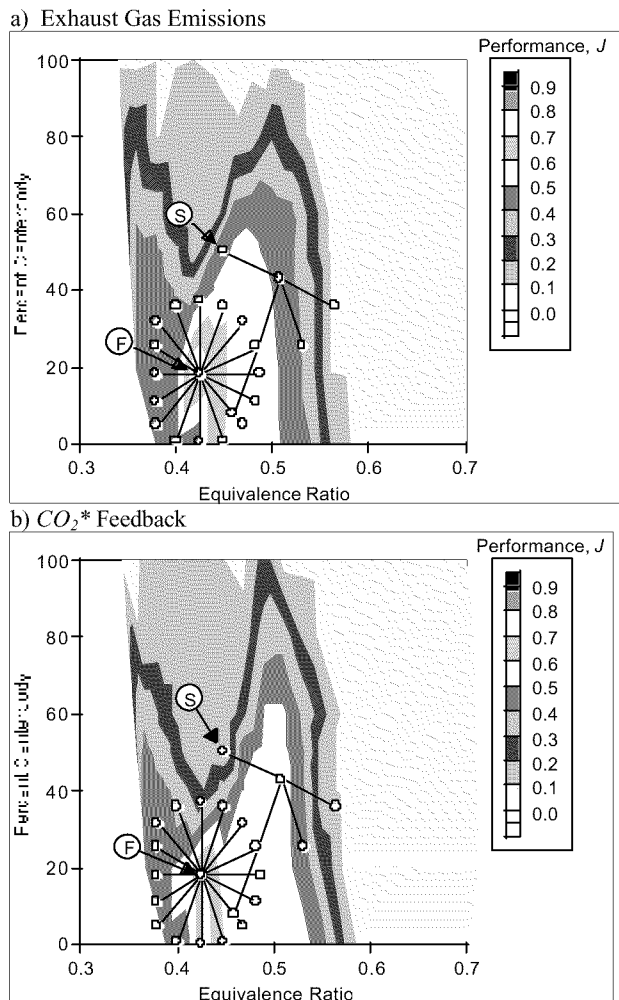


Figure 12: Optimization History for Partially Blocked Injector.

DISCUSSION

Although not illustrated previously, the differences between the actual performance (NO_x and CO emissions) and the inferred measurement (CO_2^* chemiluminescence) can obviously affect the optimization results. The correlations used in the previous optimizations were known *a priori* from detailed measurements. For practical purpose, it would be desirable to have a general sensor which can determine performance in the absence of *a priori* knowledge. Figure 13 presents the correlations between the chemiluminescence and the gaseous emissions. In contrast to Figure 6, more scatter is observed in Figure 13. This could be due to a variety of factors, including the condition of the quartz, the relative asymmetry associated with the reaction generated by the partially blocked injector. As a result, despite the apparently robust relationship between the emissions and the chemiluminescence shown for the baseline, the relationship does not hold up in general. Note that, the NO_x correlation appears to be less sensitive than the CO correlation. It could be argued that chemiluminescence levels should be greater as temperature (and as a result, NO_x) increases. Hence the generally well behaved NO_x response might be expected. CO, on the other hand has no expected relationship to

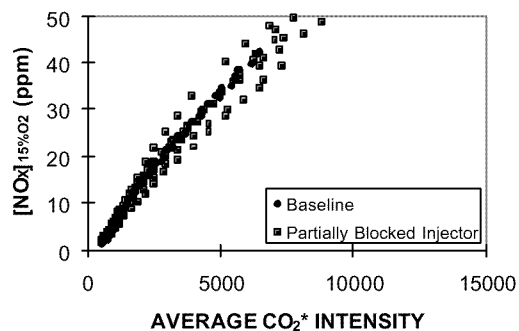
the chemiluminescence. The fluctuating chemiluminescence intensity may be related to packets of reaction which are quenched as lean blow off approaches. However, other CO formation scenarios can occur on the lean side and a trade off of mechanisms is what gives rise to the scatter shown in Figure 13b. It does bode well for the use of fluctuating chemiluminescence for stability, which has been utilized in studies looking at combustion dynamics. Additional efforts are underway to look again at the optimal location for the sensors as well as other aspects of the chemiluminescence that may allow it to be used in the absence of *a priori* knowledge of the system behavior in terms of emissions performance.

Even if *a priori* knowledge is available, the sensitivity of the strategy must be considered. If coarser, i.e., less refined, correlations were used, one wonders if the control scheme would still be able to locate the optimum regions, especially if the search (i.e., operational) space is not well-behaved, as with the hardware perturbation case. Further questions arise regarding the dependency of the optimization scheme to the initial condition and input search parameters (starting angle, increment angle, and step size). In order to begin addressing these questions, the following parameters were changed

- starting location
- starting direction, and
- CO_2^* correlations

for the hardware perturbation configuration. The results of these tests are summarized in the Table 1.

a) NO_x Correlation and Average Chemiluminescence Signal



b) CO Correlation with % Fluctuation of Chemiluminescence

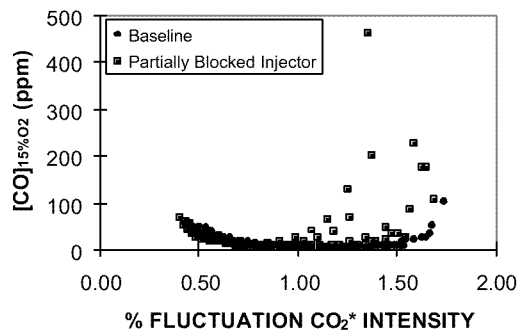


Figure 13. Total Chemiluminescence/Emissions Correlation

CONCLUSIONS

The following conclusions are offered regarding this work:

- The flexible centerbody and wall jet fuel injection strategy is able to provide sufficient mixing scenarios to allow control of the combustor performance over its entire stability range.
- The chemiluminescence sensor provides up to 2.7 times faster feedback and, therefore, allows faster optimization of the system performance.
 - The optimization, however, is dependent on the accuracy of inferential sensor correlations to characterize the actual performance parameters of NO_x and CO.
 - NO_x appears to be robustly correlated to chemiluminescence, whereas CO is not.
 - Examples are provided where coarse and fine correlations allow optimization in the correct regions. Care must be taken to accurately reflect the actual parameters of interest, and developing these without *a priori* knowledge will be challenging.
- The active optimization strategy is able to locate the high performance region of the model combustor for both the baseline firing configuration and the hardware perturbation scenario, which simulates extreme degradation or ingestion of a foreign body.
- The direction-set search algorithm employed for these initial tests is subject to many pitfalls depending on the initial search parameters (initial direction, step size, etc) and the contours of the search space (uni-modal, bi-modal, etc.).
- A stability sensor is required to allow fast, confident, and safe optimization.
- More effort is required to establish a robust correlation between inferential sensors and exhaust gas composition.

ACKNOWLEDGEMENTS

This work was funded in part by the California Energy Commission, California Institute for Energy Efficiency, the DOE Advanced Turbine Systems (ATS) program, and the Southern California Gas Company. The efforts of Mr. Steve Hill are greatly appreciated for his assistance throughout the project.

REFERENCES

- J. P. Appleton and J. B. Heywood, "The Effects of Imperfect Fuel-Air Mixing in a Burner on NO Formation from Nitrogen in the Air and the Fuel." *Fourteenth Symposium (International) on Combustion*/The Combustion Institute, 1976. pp 777-786.
- N. T. Davis and G. S. Samuelsen, Optimization of Gas Turbine Combustor Performance Throughout the Duty Cycle." *Twenty-Sixth Symposium (International) on Combustion*/The Combustion Institute, 1996. pp 2819-2825.
- R. M. Flores, M. M. Miyasato, V. G. McDonell, and G. S. Samuelsen, "Response of a Model Gas Turbine Combustor to Variation in Gaseous Fuel Composition." *Journal of Engineering for Gas Turbines and Power*/ASME, 2000.
- M. D. Jackson and A. K. Agrawal, "Active Control of Combustion for Optimal Performance." *Journal of Engineering for Gas Turbines and Power*/ASME, vol. 121, 1999. pp. 437-443.
- J. G. Lee, B. S. Hong, K. Kim, V. Yang, D. Santavicca, "Optimization of Active Control Systems for Suppressing Combustion Instability." *Symposium on Gas Turbine Engine Combustion, Emission, and Alternative Fuels*/RTO – Applied Vehicle Technology Panel, Lisbon, October 12-16, 1998.
- V. Lyons, "Fuel/Air Nonuniformity – Effect on Nitric Oxide Emissions." *AIAA Journal*, vol. 20, N5, 1981. pp. 660-665.
- Y. Neumeier and B. T. Zinn, "Experimental Demonstration of Active Control of Combustion Instabilities Using Real-Time Modes Observation and Secondary Fuel Injection." *Twenty-Sixth Symposium (International) on Combustion*/The Combustion Institute, 1996. pp 2811-2818.
- W. P. Shih, H. G. Lee, and D. A. Santavicca, "Stability and Emissions Characteristics of a Lean Premixed Gas Turbine Combustor." *Twenty-Sixth Symposium (International) on Combustion*/The Combustion Institute, 1996. pp 2771-2778.
- D. St. John and G. S. Samuelsen, "Active, Optimal Control of a Model, Natural Gas-Fired Industrial Burner." *Twenty-fifth Symposium (International) on Combustion*/The Combustion Institute, 1994. pp. 307-316.

Table 1: Sensitivity Assessment.

Parameter Change	Findings	Implications	Search History
<p><i>Starting Condition:</i></p> <p>Placed in region far from optimum in poorly performing "valley"</p>	<p>Emissions feedback, located optimum region</p>	<p>Success dependent on algorithm and initial parameters; also emissions feedback is lengthy process</p>	
<p><i>Initial Direction:</i></p> <p>Initial angle pointed in worsening direction</p>	<p>Emissions feedback (not shown) located optimum region</p> <p>CO₂* feedback (shown) optimized on a local peak and "missed" higher performance region</p>	<p>Common detriment to direction-set algorithm</p> <p>Altering step size would increase chances of "hitting" on peak region</p> <p>Inaccurate CO₂* correlation contributed to local peak optimization</p>	
<p><i>Correlation Accuracy:</i></p> <p>Coarser correlations used to derive NO_x and CO from CO₂* chemiluminescence</p>	<p>CO₂* feedback the located optimum region in twelve iterations, but took a greater number of iterations to arrive at a peak</p>	<p>Inferential methods may not need high accuracy but must accurately reflect the performance trends</p>	
<p><i>Correlation Accuracy and Initial Direction</i></p> <p>Coarser correlations and initial angle pointing in worsening direction</p>	<p>CO₂* feedback located optimum region</p>	<p>No stability parameter was included which may have altered search path away from lean limit</p>	

This page has been deliberately left blank



Page intentionnellement blanche